Atomistic simulation of the atomic structure and diffusion within the core region of an edge dislocation in aluminum

Q. F. Fang and R. Wang
Laboratory of Internal Friction and Defects in Solids, Institute of Solid State Physics, Chinese Academy of Sciences, Hefei 230031, China

(Received 28 September 1999; revised manuscript received 9 March 2000)

The core structure of an edge dislocation in aluminum is studied by molecular dynamics simulation with the glue potential. The edge dislocation of the $\frac{1}{2}[\bar{1}10](111)$ type is observed to dissociate into two partials separating from each other by a distance of 9 Å. The half width of the two partial dislocations is deduced to be 6.5 Å, giving a half width of the whole dislocation of 12 Å. Dislocation mobility is studied by applying a shear stress on the crystal and by observing the corresponding shift of the Burgers vector density. After considering the mirror force on the dislocation exerted by the fixed boundaries, a Peierls stress of $0.75\times10^{-4}\,\mu$ (μ is the shear modulus) for the motion of the whole dislocation is obtained. Atomic diffusion in the core region of the edge dislocation is simulated by hyper molecular dynamics method and the migration energy for vacancy diffusing in the dislocation core is calculated to approximate 0.5 eV.

I. INTRODUCTION

Molecular dynamics (MD) simulation is a very useful tool in the study of defect structure and atomic diffusion in crystal.[1] The atomic structures of dislocation core in metals[2–5] and in intermetallic compounds[6–8] were investigated by MD simulation in the past decade. In all studies, the phenomenon that the dislocation dissociates into two partials was observed. But the details of the dissociation obtained from the simulation depend greatly on the interatomic potential that governs the movement of the atoms to be simulated. The only way to determine which interatomic potential is most suitable is to compare the results simulated from different potentials with experimental and analytical conclusion.[9] Due to the high stacking fault energy and many body effects, simulation of the core configuration of a dislocation in aluminum is more difficult than in other fcc metals, where all pair potentials and many embedded atom methods (EAM) potentials seem to be commonly problematic.[2] For the present investigation, the so-called glue potential for aluminum suggested by Ercolessi and Adams[10] is proved to be a good choice, which can simulate the intrinsic stacking fault energy as high as 108 mJ/m^2, much higher than the values deduced from EAM potentials.

The Peierls stress subjected by a moving dislocation is determined not only by the materials parameters, but also by the atomic configuration of the dislocation core. The values of Peierls stress for fcc metals obtained from experiments or from theoretical calculations scatter in the range of 10^{-5} to $10^{-4}\mu$ where μ is the shear modulus. Kosugi and Kino[11] observed a new internal friction peak at 11 K in aluminum and attributed this peak to the mechanism of kink pair formation. They thus deduced a Peierls stress of $3\times10^{-5}\mu$. Kogure and Kosugi[4] checked the Peierls stress in copper and silver by MD simulation and obtained a Peierls stress of $3\times10^{-5}\mu$ in copper. These results are a little smaller than the general experimental results[12] but they are in agreement with that calculated from the first principle based on Peierls-Nabarro model.[13]

Simulation of the diffusion process of atoms or vacancies in lattice and in the region of defects at high temperature is also a great advantage of MD simulation. For example, Plimpton and Wolf have simulated the self-diffusion in bulk and in the grain-boundary in aluminum[9] and Huang *et al.* have simulated the pipe diffusion along a dissociated edge dislocation in copper.[14] For the pipe diffusion along dislocations the direct experimental data are difficult to obtain. The discussion of pipe diffusion is mostly based on tracer diffusion experiments carried out on low-angle grain boundaries, and only sparse results have been obtained on isolated dislocation by assuming that the dislocation has a homogeneous core of radius $\delta\approx5$ Å with high diffusivity.[15] Therefore the atomic simulation of pipe diffusion along dislocations is very important in this sense. At low temperature however, the MD method is less effective than the Monte Carlo method due to the long simulation time, but the Monte Carlo method is less direct in the simulation of atomic diffusion than the MD. Since a new MD method was suggested by Voter,[16] which was called by him the hyper-MD method, the diffusion process even at room temperature or lower can be successfully simulated by hyper-MD method.

In this paper, we have simulated the core structure of an $\frac{1}{2}[\bar{1}10](111)$ edge dislocation and the migration of vacancy in aluminum by adopting the glue potential.[10] For comparison, the core structure of the edge dislocation is also simulated by an EAM potential.[17] The interatomic potential and the simulation method are illustrated in Sec. II. The dislocation core structure and its dissociation into two Shockley partials are elucidated in Sec. III. In Sec. IV the Peierls stress is deduced from the relationship of dislocation displacement with the externally applied shear stress. The migration energy for vacancy diffusion in the core region of the edge dislocation is given in Sec. V. Finally in Sec. VI we concluded the simulation results.

II. INTERATOMIC POTENTIAL AND SIMULATION METHOD

The glue potential suggested by Ercolessi and Adams[10] and the EAM potential suggested by Mei and Davenport[17]

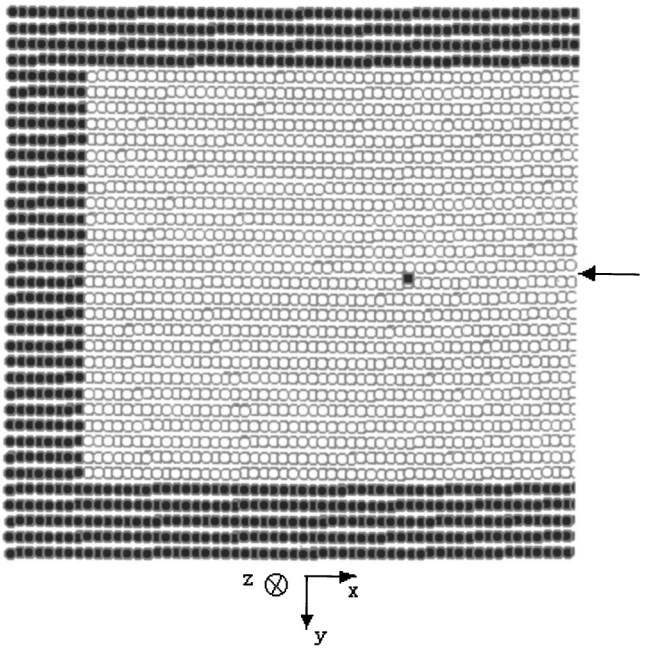

FIG. 1. A part of the model crystal with a fixed boundary (solid circles) and an edge dislocation at the center (the solid square). The atoms to be simulated are represented by open circles and the arrow indicates the position of the slip plane.

have the following general form:

$$V=\sum_i F(\rho_i)+\frac{1}{2}\sum_{\substack{i,j\\ i\neq j}} \phi(r_{ij}), \tag{1}$$

$$\rho_i=\sum_{j(\neq i)} f(r_{ij}), \tag{2}$$

where V is the total potential energy of the system, ρ_i is the electron density at the position of atom i due to all neighbor atoms, $f(r_{ij})$ is the electron density at the position of atom i due to atom j as a function of their distance r_{ij}, $\phi(r_{ij})$ is a pair potential, and $F(\rho_i)$ is a function that depends on the lattice structure and represents the many-body interaction. The two potentials differ in the actual forms of function $F(\rho_i)$, $f(r_{ij})$, and $\phi(r_{ij})$. These three functions have a simple analytical form for the EAM potential, while for the glue potential they are obtained by a numerical optimization procedure, or in other word, by combining a large amount of output of first-principle calculations (positions and forces) with traditional fitting on experimental quantities.

The cross section of the model crystal or the simulation box is shown in Fig. 1, where a $\frac{1}{2}[\bar{1}10](111)$ edge dislocation along the $[\bar{1}\bar{1}2]$ direction (perpendicular to the paper) is indicated at the center by the solid square, and the slip plane is horizontal as pointed to by the arrow. The total atom numbers in the model crystal can reach more than 10 000 in the simulation of dislocation core structure. In the simulation of diffusion and dislocation slip, the total number counts 5736 with the number of movable atoms being 3380. Periodic boundary condition is applied along the dislocation line but the boundaries along the other two directions ($[\bar{1}10]$ and $[111]$) are fixed (the solid circles in Fig. 1 represent the position of the fixed boundary atoms). The fixed boundary will affect the dislocation core structure and the dynamics of the atoms in the core region. However, this effect can be neglected if the simulation box is large enough, as in our case where the dimensions of the simulation box in the directions of $[\bar{1}10]$ and $[111]$ is more than 30 times of Burgers' vector.

To prepare this configuration, an ideal fcc lattice with a lattice constant of 4.03 Å is first constructed with the lattice vectors x ($[\bar{1}10]$), y ($[111]$), and z ($[\bar{1}\bar{1}2]$) along the edges of the simulation box. Then all atoms are displaced according to the linear isotropic elastic theory to produce an edge dislocation at the center, and the overlapped atoms after the displacement are removed. At last the system is relaxed so that each atom feels no force. This relaxation process is realized by moving each atom according to Newton's equations of motion and setting the velocity of every atom to zero after each time step in the aim to quickly equilibrate the atoms.[18] This process proceeds until the absolute value of the spatial derivatives of the total potential energy becomes smaller than a given positive number, i.e., until $|\vec{\nabla}V|^2<2.5\times10^{-5}\,(\mathrm{eV/\AA})^2$.

To investigate the mobility of an edge dislocation under a shear stress, a dynamic simulation is performed. A shear stress is applied on the slip plane (111) along the slip direction $[\bar{1}10]$. To produce such a shear stress in the lattice, all atoms including those in the boundary region are displaced according to the strain field corresponding to this shear stress. According to the linear elastic theory, the shear stress τ is associated with the strain or the shear angle θ as $\tau=\mu\tan\theta$. So the model crystal is sheared by θ to maintain a shear stress in it.

According to Peierls-Nabarro model[12] a gliding dislocation feels a periodical potential. Peierls stress is defined as the maximum stress needed for the dislocation to overcome this periodical potential. The fixed boundary will exert inevitably an image force on the dislocation, which can be assumed to have a linear relationship with the dislocation displacement in the case of small displacement.[12] By considering the image force and Peierls stress together, the relation between the shear stress and the dislocation displacement can be written in the following form:

$$\tau(u)=Ku+\tau_1\sin\left(\frac{2\pi u}{d}\right)+\tau_2\sin\left(\frac{4\pi u}{d}\right), \tag{3}$$

where $\tau(u)$ is the shear stress, u is the dislocation displacement, K is a constant representing the magnitude of the image force, d is the period of the Peierls energy, which we choose to be 2.85 Å, the same as the Burgers vector, τ_1 and τ_2 are constants. The last term in Eq. (3) is added because the perfect dislocation of $\frac{1}{2}[\bar{1}10](111)$ will pass a metastable position at the middle point of the slip distance d, or the Peierls potential has a local minimum. The Peierls stress can be obtained as the maximum value of the sum of the last two terms in Eq. (3). Therefore, if we calculate the variation of shear stress with the equilibrium position of the dislocation, we can obtain the Peierls stress according to Eq. (3). To do this, it is necessary to accurately determine the equilibrium position of the dislocation under different shear stresses, which is not easy in the case of high shear stress. The

method adopted by Kogure and Kosugi,[4] in which the dislocation is assumed to have reached its equilibrium position when the kinetic energy of the system has just reached its maximum, is not accurate enough in our case. So we present a new approach as following, which is proved to be more accurate.

After the deformation, each movable atom is given a random velocity to raise the temperature of the crystal to 101 K or higher. A dynamic simulation is performed by keeping the atom number, crystal volume, and the temperature constant. This simulation method proposed by Brown and Clarke[19] is consistent with the canonical ensemble. The temperature of the system is decreased after every 500 time steps by 10 K, until the temperature reaches to 1 K. The total energy of those moving atoms is then minimized using a conjugate-gradient technique, allowing each atom to reach to its equilibrium position. To determine the position of the dislocation, the function of Burgers vector density is introduced, which is defined as the spatial derivative of the x component of the relative displacement at the slip plane with the x coordinate. The position where the Burgers vector density has a maximum as a function of x is defined as the center of the dislocation.

The hyper-MD simulation method[16] is a general method for accelerating the MD simulation of infrequent events in solids, for example atomic diffusion, on the basis of the transition state theory. A bias potential ΔV raises the energy in regions other than the transition states between potential basins. The superposition of this bias potential will make the total resultant potential valley shallower and shorten the time interval for the atoms to stay at the valley. Transitions occur at an accelerated rate and the elapsed time becomes a statistical property of the system. This ΔV is computationally constructed without the advance knowledge of the potential surface, but must be zero at the saddle points of the potential so that the atomic diffusion is enhanced while not changing the diffusion mechanism. According to Voter, the time scale is enlarged nonlinearly when a bias potential ΔV is added:

$$\Delta t_{\mathrm{bi}} = \Delta t_{\mathrm{MD}} \exp\left(\frac{\Delta V_i}{kT}\right), \tag{4}$$

where k is the Boltzmann constant, T is the absolute temperature, ΔV_i is the bias potential at the ith time step, Δt_{bi} and Δt_{MD} are the escaped real time at ith step and the MD time step, respectively. In our case, we choose $\Delta t_{\mathrm{MD}} = 2 \times 10^{-15}$ sec. The total real time is thus

$$t_b = \sum_{1}^{n} \Delta t_{\mathrm{bi}}, \tag{5}$$

where n is the total number of MD time steps.

The ΔV is in general a function of all atoms to be simulated, and thus its calculation is much time consuming, especially for a large number of simulating atoms. Gong and Wilkins[20] improved this hyper-MD by localizing the ΔV on some selected atoms. This localization approximation can be viewed as dividing the system into two subsystems with different interatomic potential. Although only a few atoms' movement can be accelerated, this improved method will simplify the calculation of ΔV and save much computation time. This local hyper-MD method is very suitable to study the dynamics of a group of atoms while the dynamics of other atoms is not in interest, for instance, in the case of surface diffusion of adatom and dimer. However, for the study of the dynamics of whole system, as in the case of phase transition, this simplified method will not be applicable and we must consult to the original method suggested by Voter.

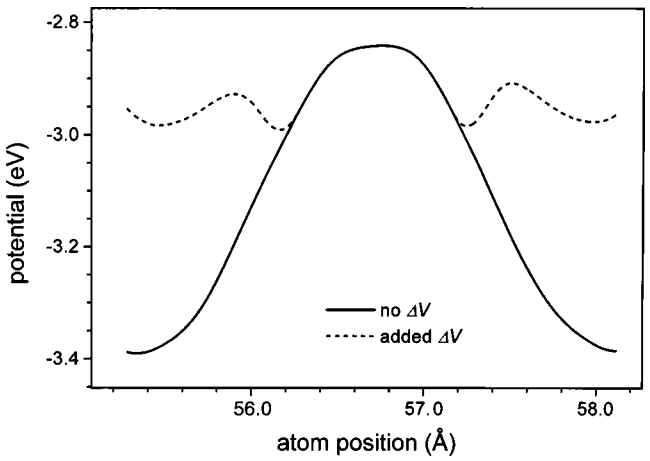

FIG. 2. The potential profile of the selected atom without bias potential ΔV (solid line) and with bias potential ΔV (dashed line). The potential valley is nearly filled up by ΔV.

The choice of the function form for ΔV is arbitrary as long as the ΔV is zero at the saddle points of the potential ($\nabla V = 0$) and there would be no deeper valleys after the addition of ΔV. In the following simulation of vacancy diffusion in dislocation core, we follow the local hyper-MD method, but localize the bias potential ΔV only on one selected atom and construct ΔV according to the following formula, which is a combination of the two forms of ΔV suggested by Voter:[16]

$$\Delta V = \frac{z}{1 + z/z_{\max}}; \quad z = a\,\theta(\varepsilon_1 - \varepsilon_{\mathrm{base}})(\varepsilon_1 - \varepsilon_{\mathrm{base}})^2, \tag{6}$$

where a, $z_{\max}$, and $\varepsilon_{\mathrm{base}}$ are tunable parameters, θ is the standard step function, ε_1 is the minimum eigenvalue of the Hessian matrix H ($H_{ij} \equiv \partial^2 V / \partial x_i \partial x_j$), which has the size of only 3×3 in our case. The introduction of parameters $z_{\max}$ and $\varepsilon_{\mathrm{base}}$ is to control the maximum value of ΔV and to enhance the acceleration effect, respectively, and the choice of their values depends on the characteristic of the potential. By localizing ΔV on only one selected atom and creating a vacancy in the neighboring, we can study the orientation dependence of the diffusion coefficient for the dislocation core diffusion.

In the simulation we choose $z_{\max} = 0.6$ eV for bulk diffusion and $z_{\max} = 0.5$ eV for dislocation core diffusion, and $a = 0.5\,\text{Å}^4/\text{eV}$, $\varepsilon_{\mathrm{base}} = 0.9\,\text{eV}\,\text{Å}^2$ for both cases. These parameter values are adjusted by comparing the potential profiles of the selected atom before and after the addition of the bias potential ΔV, as shown in Fig. 2, where the solid line represents V and the dash line is $V + \Delta V$ of the selected atom in the dislocation core. The curves in Fig. 2 are calculated from Eqs. (1), (2), and (6) using the above parameter values, when the selected atom moves quasistatically from one vacant site

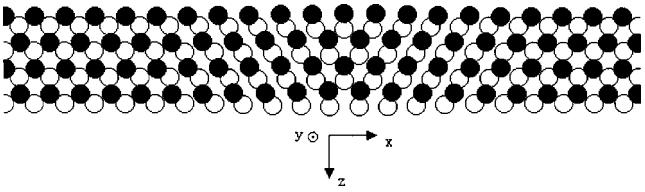

FIG. 3. Atomic structure in the core region of the edge dislocation. The dislocation line lies in the plane of the paper along the vertical direction and the Burgers' vector is along the horizontal direction.

to the neighboring vacant site. By adding a bias potential described in Eq. (6), the original valley of about 0.55 eV is nearly filled up, leaving shallower valleys of only 0.1 eV. This will greatly enhance the atomic diffusion.

III. CORE STRUCTURE OF AN EDGE DISLOCATION

The core structure of the dislocation obtained with the above procedure is shown in Fig. 3, where the dislocation line is along z axis and the Burgers vector is along the x axis. The solid and open circles represent the atoms in the two neighboring slip planes adjacent to the dislocation line, respectively. The solid circles are the atoms in the dilatation region at the lower slip plane while the open circles are the atoms in the compression region at the upper slip plane. The misfit in the core region is apparent and spreads several atomic spacing wide.

By comparing the positions of the corresponding atoms at the two neighboring slip planes, we can obtain the relative displacement of the atoms. The x and z components of this displacement as a function of the x coordinate are shown in Fig. 4. The x component is zero at one end, and at another end is 2.85 Å, equal to the magnitude of the Burgers' vector. The region where the x component dramatically changes represents the dislocation core region. The z component has a nonzero value only in the dislocation core, the maximum of which is about 0.45 Å at the center of the dislocation core. This nonzero z component of displacement reflects the dislocation dissociation, because only in a dissociated dislocation the atoms displace along the direction of $[\bar{1}2\bar{1}]$ instead

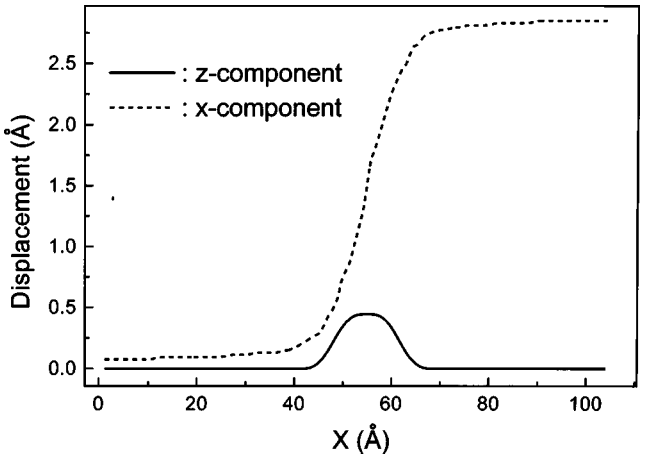

FIG. 4. The x component (dotted line) and z component (solid line) of the relative displacement of atoms as a function of the x coordinate (in the direction of Burgers' vector).

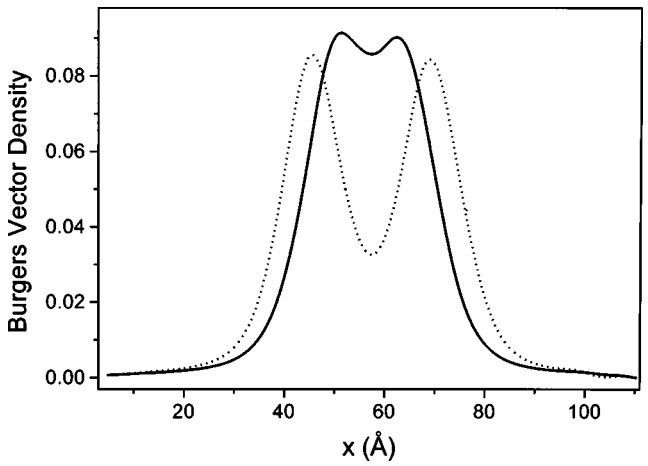

FIG. 5. the Burgers vector density obtained by simulation with the glue potential (solid line) and with the EAM potential (dotted line).

of $[\bar{1}10]$. It is worth noting that the maximum value of the z component is much smaller than the projection on the z coordinate of the Burgers' vector of the Shockley partial $\frac{1}{6}[\bar{1}2\bar{1}]$, which is equal to 0.82 Å. This fact suggests that the area within the dissociated dislocation is not a pure stacking fault ribbon, where the core regions of the two partials overlap and the z components of their displacements annihilate with each other.

The Burgers vector density as functions of x obtained by the simulation with the glue potential (solid line) and with the EAM potential (dotted line) is shown in Fig. 5. There are two peaks representing the centers of the two Shockley partials. The separation distance between the two partials obtained by the EAM potential is about 30 Å, which is unreasonably large but close to the result obtained previously by Häkkinen *et al.*[2] However, a much smaller separation distance of about 9 Å is obtained by using the glue potential.

According to the elastic theory, the separation distance of the two partials is

$$r_e=\frac{G_{\langle 111\rangle}b_2{}^2(2+\nu)}{8\pi\gamma_1(1-\nu)}, \tag{7}$$

where b_2 is the Burgers vector of the partial dislocations, γ_I is the intrinsic stacking fault energy, ν is the Poisson's ratio, $G_{\langle 111\rangle}$ is the shear modulus across the (111) plane that can be written as $G^{-1}_{\langle 111\rangle}=\frac{1}{3}C^{-1}_{44}+\frac{4}{3}(C_{11}-C_{12})^{-1}$ in fcc materials with C_{11}, C_{12}, C_{44} being elastic constants. The values of the above parameters for Al obtained from experiment and calculated from the glue potential are listed in Table I. Using the parameter values from glue potential, the separation distance between the two partials can be calculated as $r_e=11.2$ Å according to Eq. (7), which is close to the value of 9 Å simulated by the glue potential. This coincidence between the simulation result and the prediction of the elastic theory indicates that although the separation between two partial dislocations is only three times of the Burgers vector, the interaction laws between dislocations predicted by elastic theory are still applicable. The present equilibrium separation between the two partials (9 Å) is relatively small among those ever obtained in the atomistic simulation of the dislo-

TABLE I. Values of parameters used in Eq. (7).

	b_2^2 (Å^2)	C_{11} (10^{10} Pa)	C_{12} (10^{10} Pa)	C_{44} (10^{10} Pa)	C_{111} (10^{10} Pa)	γ_l (J/m^2)	ν
By glue potential	2.71	11.81	6.24	3.67	3.302	0.108	0.320
Experimental		10.82	6.13	2.85	2.492	0.166	0.347

cation core structure in Al, similar with the results obtained by Aslanides and Pontikis,[21] although it is much larger than the separation of 5.8 Å estimated from Eq. (7) by using the parameter values from experiment.

To determine the half width of the dislocation, the Burgers vector density in Fig. 5 for the glue potential is fitted into the derivative function of the arctangent function. This function has the form of $P\xi^2/[(x-x_0)^2+\xi^2]$, where P is the peak height, x_0 and ξ are the center and the half width of the dislocation core, respectively. The obtained half width of the partials is 6.5 Å. The half width of the whole dislocation is thus 12 Å including the stacking fault ribbon. This is to say, if the dislocation in aluminum is treated as a whole dislocation, its half width is almost four times of the Burgers vector.

IV. PEIERLS STRESS—MOBILITY OF THE EDGE DISLOCATION

When a shear stress is applied on the crystal and a dynamic simulation with the approach presented above is performed, the dislocation changes its position accordingly, as shown in Fig. 6, where a shear stress of $2\times10^{-3}\,\mu$ is applied on the model crystal. The original Burgers vector density is the dotted curve, while the solid curve represents the Burgers vector density under the action of the shear stress. It can be seen clearly that the dislocation glides along the direction of the shear stress. The separation distance between two partials keeps almost constant in the gliding process, that is to say, although it dissociated into two partials, the dislocation glides as a whole when a shear stress is applied on its slip plane. By changing the magnitude of the stress, the relationship between the dislocation displacement and the shear stress is obtained as shown in Fig. 7. The solid squares in Fig. 7 are results obtained by the simulation, and the solid line is the result obtained by a numerical least-square fitting on the solid squares using Eq. (3). The parameters K, τ_1, and τ_2 in Eq. (3) are fitted to be $6.5\times10^{-4}\,\mu$/Å, $0.75\times10^{-4}\,\mu$, and $-0.11\times10^{-4}\,\mu$, respectively.

It can be seen from Fig. 7 that the fitted line and the solid squares are generally well consistent with each other. The fitted sinusoidal part (the Peierls stress) is enlarged and shown in the inset of Fig. 7. The higher order term in $\sin(2\pi u/d)$ in Eq. (3) (the last term) plays a much smaller role than the term $\sin(2\pi u/d)$. It is clear that the amplitude of the sinusoidal function or the Peierls stress is equal to $0.75\times10^{-4}\,\mu$. This value of Peierls stress is comparable with the general experiment[12] and nearly two times larger than the result of Kosugi and Kino.[11]

V. VACANCY DIFFUSION IN THE DISLOCATION CORE

In the case of fixed boundary, only Frenkel pairs (vacancy and self-interstitial atom) can be created if the simulation process lasts long enough. Because of the large formation energy of Frenkel pairs, vacancies cannot be automatically created in the simulation process that lasts for only several hundreds of ps, as in the case of grain boundaries. Therefore it is necessary to introduce a vacancy into the lattice or into the dislocation core before the diffusion can start. In fact we observed no successful jump of the atom when no vacancy initially exists. With an enhancement of diffusion, the selected atom will jump into the neighboring vacant site after having vibrated at its equilibrium position for some time.

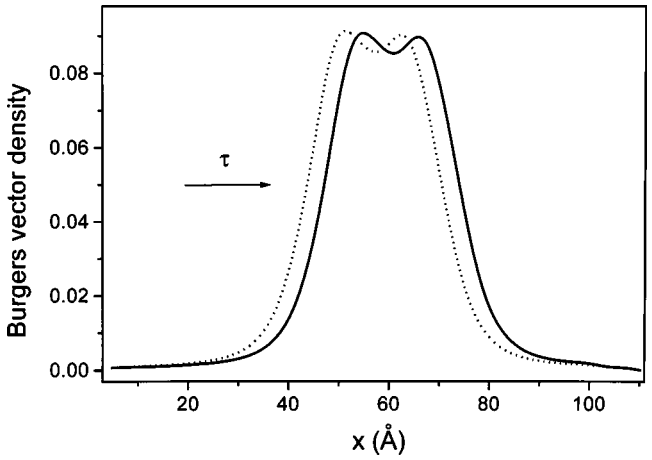

FIG. 6. The movement of the dislocation under shear stresses. The dotted line indicates the original position of the dislocation; the solid line indicates the dislocation position after the shear stress is applied.

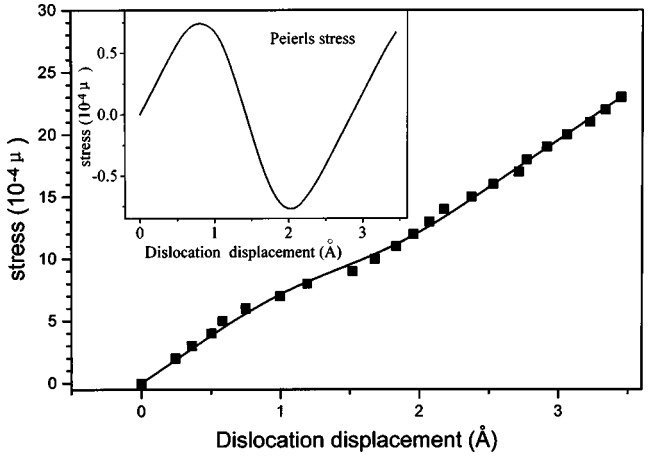

FIG. 7. The relationship of the shear stress with the dislocation displacement. The solid squares are obtained by molecular dynamics simulation; the solid line is the least-square fitting of the simulation data into Eq. (3). The inset is the enlargement of the sinusoidal part, showing a Peierls stress of $0.75\times10^{-4}\,\mu$.

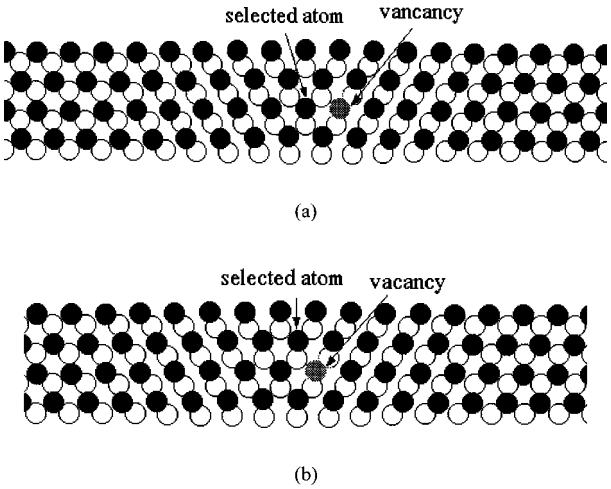

FIG. 8. Schematic diagrams illustrating the introduction of vacancies and the selection of the trace atom. The dislocation line lies in the plane of the paper along the vertical direction. (a) Configuration for transverse core diffusion; (b) configuration for longitudinal core diffusion.

When the simulation process continues, the selected atom will jump between these neighboring sites initially occupied by the selected atom and the vacancy. This forth and back jump process of the selected atom is the same process when we view that the vacancy makes such forth and back jumps. So we actually simulate here the migration process of vacancy.

Since we can only simulate the diffusion process of one selected atom by adopting the local hyper-MD method as mentioned above, the position of the introduced vacancy relative to the selected atom will determine the diffusion direction. This diffusion direction will not matter for the bulk diffusion simulation because the fcc aluminum lattice is homogeneous. For the pipe diffusion simulation however, the diffusion coefficient or activation energy will be different when the vacancy diffuses along different direction relative to the dislocation line. The experimental researches on the internal friction peaks in cold-worked Al-Mg alloys,[22] which are proposed to be associated with the atomic readjustment in the dislocation core, have shown that the activation energy for transverse core diffusion (TCD) is larger than for longitudinal core diffusion (LCD). The diffusion direction for TCD is perpendicular to the dislocation line but in the slip plane while for LCD it is parallel to the dislocation line. We construct the initial configurations as shown in Fig. 8, with the connecting direction from the selected atom to vacancy perpendicular to the dislocation line [Fig. 8(a), for TCD] or having an angle of 30° relative to the dislocation line [Fig. 8(b), for LCD]. The vacancy is introduced into the dilatation region where the pipe diffusion is believed to be easier than in the compressive region and in the lattice.

As an example, The displacement of the selected atom (or vacancy vice versa) versus time steps when it diffuses longitudinally along z direction in the dislocation core is shown in Fig. 9, which is obtained in a pipe diffusion simulation at 400 K by the hyper-MD. It can be seen clearly that the selected atom or the introduced vacancy jumps between the two neighboring equilibrium sites. In the most part of the simulation period, the vacancy vibrates in the vicinity of one

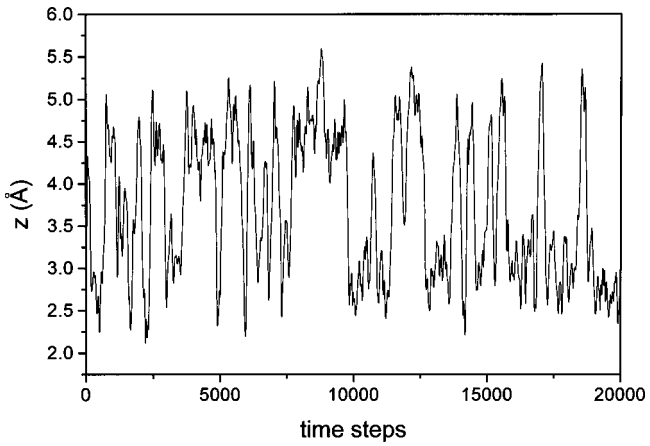

FIG. 9. The displacement of the selected atom versus time steps when it diffuses longitudinally along z direction in the dislocation core, which is obtained in a pipe diffusion simulation at 400 K by the hyper-MD.

equilibrium site, and only 35 successful jumps occur in the whole simulation period of 40 ps. However, the real time elapsed in the simulation process is enhanced by a factor of 10 000 in average in virtue of the hyper-MD, as calculated from Eq. (4). That is to say, in a period of about 400 ns there are 35 jumps for vacancy longitudinally diffusing in the dislocation core.

By counting the numbers of successful jumps N and calculating the real elapsed time t_b from Eqs. (4) and (5), the jump rate can be calculated at different temperature as $\Gamma = N/t_b$. We assume here that Γ has an Arrhenius relation with temperature $\Gamma = \Gamma_0 \exp(-H_m/kT)$ not only in the bulk but also in the dislocation core region, where H_m is the migration energy of vacancies and Γ_0 is a constant. Then we can obtain the quantity H_m by plotting the values of $\ln(\Gamma)$ versus the reciprocal of temperature. These Arrhenius plots of $\ln(\Gamma)$ versus $1/T$ are shown in Fig. 10 for bulk diffusion (△), LCD (○), and TCD (□) of vacancies. The vacancy migration energies for bulk diffusion (H_m^b), LCD (H_m^L), and

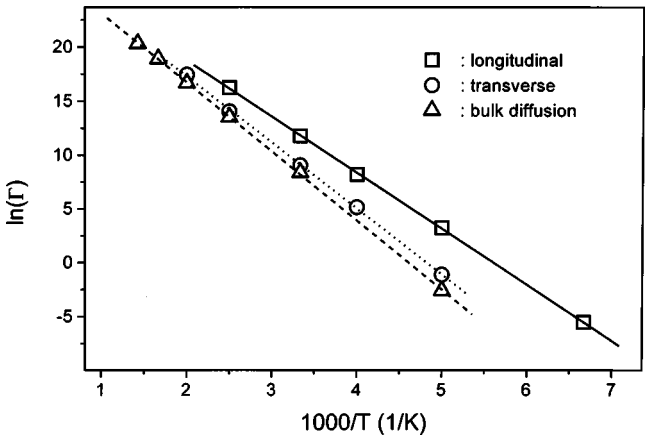

FIG. 10. The plots of $\ln(\Gamma)$ versus the reciprocal of temperature. The symbols are the simulated results for bulk diffusion (△), longitudinal (○), and transverse (□) diffusion in the dislocation core for a vacancy. Least-square fitted lines yield vacancy migration energies of 0.55, 0.45, and 0.53 eV, respectively, for bulk, longitudinal, and transverse diffusions.

TCD (H_m^T) deduced from the slope of the lines in Fig. 10 are 0.55, 0.45, and 0.53 eV, respectively. It is worth to point out that H_m^L and/or H_m^T are smaller than H_m^b. It is also interesting to note that H_m^T is larger than H_m^L, which is in accordance with the prediction of internal friction study.[22] This effect that LCD is easier than TCD was also observed in Al by Hoagland *et al.*[23] at elevated temperature by using Monte Carlo simulation with the same glue potential, where they designated the TCD and LCD as radial and *z* component, respectively. However, the average migration energy of a vacancy in dislocation core that they have obtained as 0.34 eV is much smaller than the present results. This discrepancy may come from the different simulation methods, since the H_m^b simulated by these two methods are also different and between them lies the experimental data of 0.6 eV for vacancy migration energy in Al.[24] At present we argue that our results may be more reliable, because the migration energy of vacancy for pipe diffusion is comparable to H_m^b with a ratio of 0.89, which is similar with the result of 0.94 in copper[14] where they did not distinguish between TCD and LCD.

As suggested by Balluffi and Granato,[25] the formation energy of vacancies in the dislocation core would be the half of that in bulk and is about 0.35 eV in Al, by using the vacancy formation energy of 0.69 eV in the bulk predicted by glue potential.[10] Combining this value and our simulation results, we can obtain the activation energy for TCD and LCD as 0.88 and 0.8 eV respectively, which are in good agreement with the experimental data of 0.85 eV measured from mass transport along dislocation by capillarity.[26] The activation energies of Mg atoms for TCD and LCD in Al deduced from internal friction peak in Al-Mg alloys are 0.6 and 0.5 eV, respectively,[22] which are comparable with the migration energy of vacancy in dislocation core. This fact suggests that in the case of the internal friction measurement in cold-worked Al-Mg alloys, there may be enough vacancies existing initially in the core region so that the diffusion of the atoms in dislocation core needs not to form vacancies at first. This suggestion is reasonable because in addition to the attraction of the dislocation, the vacancy is attracted by the Mg atoms in the dislocation core due to the especially large binding energy between vacancy and Mg atom.[27] The results obtained in Al-Cu alloys where the Cu atom has a smaller binding energy with vacancies support this suggestion further. The activation energy of Cu atom diffusing in the dislocation core region in Al-Cu alloys is deduced from the similar internal friction peak to be 0.8 eV,[28] similar with that for the self-diffusion in the dislocation core.

We can see the validity of the localized hyper-MD in a reasonable sense from the simulated values of H_m^b and Γ_0. The Γ_0 is the vibration frequency of the vacancy at the equilibrium sites, usually close to Debye frequency in solids. The Γ_0 for the bulk diffusion, LCD and TCD obtained from Fig. 10 are almost same and in the magnitude order of $10^{13}\,\mathrm{sec}^{-1}$, consistent with the Debye frequency. This illustrates that the addition of the bias potential ΔV in the localized hyper-MD almost did not affect Γ_0. The bulk migration energy of vacancy in Al (H_m^b) simulated by hyper-MD is 0.55 eV, comparable to the result of 0.61 eV predicted by the glue potential.[10] This fact shows that we can obtain reliable parameters for atomistic diffusion both in bulk and in the defect region by using the approach of localized hyper-MD and the parameters adopted in present work. A complete check of the validity of the localized hyper-MD approach may be to simulate the atomistic diffusion by changing the ΔV in until $\Delta V \to 0$, which is planned and will be reported at a later stage.

VI. DISCUSSION AND CONCLUSION

The MD simulation method is useful in studying the defect structure and the atomic diffusion in bulk or in the region of defect. By using the newly developed hyper-MD method, one can simulate the atomic diffusion even at room temperature or lower temperature just for a relatively short simulation time. The simulation results, however, as illustrated in the Introduction, are dependent on the interatomic potential. Unfortunately, there are no absolute answers as to which potential is most suitable. For one kind of materials, we could find several interatomic potentials in the literatures. One potential will be successful for some kinds of problems, but may fail for some other problems. So we must be careful in the selection of the interatomic potential before we sit down to solve the problem by the MD simulation method.

Why the migration energy for a vacancy diffusing perpendicular to the dislocation line (TCD) is larger than that parallel to the dislocation line (LCD) can be understood on the basis of the dislocation core structure. Because the dilatation in the dislocation core extends mainly in the *x* direction (the direction of Burger's vector), the average atomic spacing will be larger in the *x* direction than in the *z* direction (along dislocation line, or exactly speaking inclined to the dislocation line with an angle of 30°). In the diffusion process the diffusing atom will repel the neighboring atoms aside and squeeze through the saddle point. So when the selected atom diffuses along the dislocation line and repels the neighboring atoms apart in *x* direction to pass through the saddle point, it will feel sparer space and pass through the saddle point more easily than when it diffuse along the *x* direction. This effect will result in smaller migration energy for LCD.

The glue potential is proved to be a satisfactory potential to describe the interatomic interaction in aluminum, especially for simulating the dislocation core structure and the atomic diffusion. The main simulation results obtained in this paper by using the MD method and the glue potential can be concluded as the following:

(1) The edge dislocation of $\frac{1}{2}[\bar{1}10](111)$ type in aluminum lattice dissociates into two Shockley partials separating from each other by a distance of about 9 Å and the half width of the partial dislocation is 6.5 Å. If we treat the edge dislocation as a whole, its half width can reach 12 Å, three times larger than the value of Burgers' vector.

(2) The *z* component of the relative displacement between the corresponding atoms in two neighboring slip planes can be used to sensitively judge the dislocation dissociation.

(3) A Peierls stress in the magnitude order of $0.75 \times 10^{-4}\,\mu$ is obtained for the whole dislocation moving in aluminum lattice, where μ is the shear modulus.

(4) The migration energies of a vacancy are obtained from simulation with hyper-MD method as being 0.55 eV for bulk

diffusion, 0.53 eV for transverse core diffusion, and 0.45 eV for longitudinal core diffusion. The fact that the migration energy for bulk diffusion is larger than for core diffusion and that the migration energy for TCD is larger than for LCD is in agreement with the results deduced from the internal friction measurements. By assuming that the formation energy of a vacancy in the dislocation core is about half of that in the bulk, i.e., 0.35 eV, we can estimate the activation energy of self-diffusion in the dislocation core as in the range from 0.8 to 0.88 eV, which is consistent with experiments.

ACKNOWLEDGMENTS

This work has been subsidized by the National Natural Science Foundation of China (Grant No. 59601008). Q.F.F. thanks G. Schoeck in University of Vienna in Austria for useful discussions.

[1] *Atomistic Simulation of Materials: Beyond Pair Potentials*, edited by V. Vitek and D. J. Srolovitz (Plenum, New York, 1989).
[2] H. Häkkinen, S. Mäkinen, and M. Manninen, Phys. Rev. B **41**, 12 441 (1990).
[3] J. Huang, M. Meyer, and V. Pontikis, Phys. Rev. B **42**, 5495 (1990).
[4] Y. Kogure and T. Kosugi, J. Phys. III **6**, C8-195 (1996).
[5] T. Rasmussen, K. W. Jacobsen, T. Leffers, and O. B. Pedersen, Phys. Rev. B **56**, 2977 (1997).
[6] R. Schroll, V. Vitek, and P. Gumbsch, Acta Mater. **46**, 903 (1998).
[7] J. Panova and D. Farkas, Philos. Mag. A **78**, 389 (1998).
[8] S. Kohlhammer, M. Fähnle, and G. Schoeck, Scrip. Mater. **39**, 359 (1998).
[9] S. J. Plimpton and E. D. Wolf, Phys. Rev. B **41**, 2712 (1990).
[10] F. Ercolessi and J. B. Adams, Europhys. Lett. **26**, 583 (1994).
[11] T. Kosugi and T. Kino, Mater. Sci. Eng., A **164**, 368 (1993); Mater. Sci. Forum **119–121**, 177 (1993).
[12] J. P. Hirth and J. Lothe, *Theory of Dislocations*, 2nd ed. (Wiley, New York, 1982), pp. 94, 240–242.
[13] J. Hartford, B. von Sydow, G. Wahnström, and B. I. Lundqvist, Phys. Rev. B **58**, 2487 (1998).
[14] J. Huang, M. Meyer, and V. Pontikis, Phys. Rev. Lett. **63**, 628 (1989); Philos. Mag. A **63**, 1149 (1991).
[15] R. W. Balluffi, Phys. Status Solidi B **42**, 11 (1970).
[16] A. V. Voter, J. Chem. Phys. **106**, 4665 (1997); Phys. Rev. Lett. **78**, 3908 (1997).
[17] J. Mei and J. W. Davenport, Phys. Rev. B **46**, 21 (1992).
[18] Setting the velocities to zero after every time step is somewhat inefficient, but it can reach equilibrium easily. A significantly better approach may be to set the velocities to zero whenever the potential energy begins to rise, but do not alter the velocities as long as the potential energy decreases [for example, refer to P. C. Gehlen, J. Appl. Phys. **41**, 5165 (1970)]. However, an additional equilibration process is required if the velocities are large before being set to zero.
[19] D. Brown and J. H. R. Clarke, Mol. Phys. **51**, 1243 (1984).
[20] X. G. Gong and J. W. Wilkins, Phys. Rev. B **59**, 54 (1999).
[21] A. Aslanides and V. Pontikis, Comput. Mater. Sci. **10**, 401 (1998).
[22] T. S. Kê, Q. Tan, and Q. F. Fang, Phys. Status Solidi A **103**, 421 (1987); Q. Tan and T. S. Kê, *ibid.* **122**, K25 (1990).
[23] R. G. Hoagland, A. V. Voter, and S. M. Foiles, Scrip. Mater. **39**, 589 (1998).
[24] A. Seeger, J. Phys. F: Met. Phys. **3**, 248 (1973).
[25] R. W. Balluffi and A. V. Granato, in *Dislocation in Solids*, edited by F. R. N. Nabarro (North-Holland, Amsterdam, 1979), Vol. 4, p. 1.
[26] T. E. Volin, K. H. Lie, and R. W. Balluffi, Acta Metall. **19**, 263 (1971).
[27] Q. F. Fang and T. S. Kê, Acta Metall. Mater. **38**, 419 (1990).
[28] A. W. Zhu and T. S. Kê, Phys. Status Solidi A **128**, 95 (1991).